

# STRUCTURE OF LOW-LYING QUADRUPOLE STATES IN NUCLEI NEAR $^{132}\text{Sn}$

A. P. Severyukhin<sup>1</sup>, V. V. Voronov<sup>1</sup>, N. N. Arsenyev<sup>1</sup>, N. Pietralla<sup>2</sup>,  
Nguyen Van Giai<sup>3</sup>

<sup>1</sup>*Bogoliubov Laboratory of Theoretical Physics, JINR, 141980 Dubna, Russia*

<sup>2</sup>*Institut für Kernphysik, Technische Universität Darmstadt, 64289 Darmstadt,  
Germany*

<sup>3</sup>*Institut de Physique Nucléaire, CNRS-IN2P3, Université Paris-Sud, F-91406  
Orsay Cedex, France*

The properties of the low-lying  $2^+$  states in the even-even nuclei around  $^{132}\text{Sn}$  are studied within the quasiparticle random phase approximation. Starting from a Skyrme interaction in the particle-hole channel and a density-dependent zero-range interaction in the particle-particle channel, we use the finite rank separable approach in our investigation. It is found that the  $2_4^+$  state in  $^{132}\text{Te}$  could be a good candidate for a mixed-symmetry state.

## 1. Introduction

The low-energy spectrum of nuclear excitations provides the most sensitive testing ground for nuclear structure calculations in the presence of pairing correlations. The evolution of the low energy spectrum in nuclei around  $^{132}\text{Sn}$  is an increasingly important point for the investigation of nuclear structure physics and nuclear astrophysics. There is a relation between the  $N = 82$  shell closure and the  $A \approx 130$  peak of the solar r-process abundance distribution, i.e., the structural peculiarities of the  $N = 82$  isotones lighter than  $^{132}\text{Sn}$  are important for the stellar nucleosynthesis. New experiments [1, 2, 3, 4, 5, 6, 7, 8, 9] give spectroscopic observations in nuclei near  $^{132}\text{Sn}$  and this is a good possibility to test theoretical approaches. One of the successful tools for nuclear structure studies is the quasiparticle random phase approximation (QRPA) with the self-consistent mean-field derived by making use of the Skyrme effective nucleon-nucleon interaction [10]. Such QRPA calculations do not require to introduce new parameters since the residual interaction is derived from the same energy density functional as that determining the mean-field. Results of calculations of the properties of the low-lying states in nuclei with very different mass numbers within this approach are in a reasonable agreement with experimental data.

Making use of the finite rank separable approximation [11, 12] for the residual interaction enables one to perform the QRPA calculations in very large two-quasiparticle spaces. Recently, we generalized our approach to take into account a coupling between the one- and two-phonon components of the wave functions [13]. Here, we

use an extension of our approach by taking into account the particle-particle (p-p) residual interaction [14].

In the present report we briefly describe our method and present the analysis of the properties of the low-lying  $2^+$  states in even-even nuclei around  $^{132}\text{Sn}$ .

## 2. The method

This method has already been presented in details in Refs. [11, 12, 14] and we only sketch it briefly here. The starting point of the method is the HF-BCS calculation [15] of the ground states, where spherical symmetry is imposed on the quasiparticle wave functions. The continuous part of the single-particle spectrum is discretized by diagonalizing the HF Hamiltonian on a harmonic oscillator basis [16]. We work in the quasiparticle representation defined by the canonical Bogoliubov transformation:

$$a_{jm}^+ = u_j \alpha_{jm}^+ + (-1)^{j-m} v_j \alpha_{j-m}, \quad (1)$$

where  $jm$  denote the quantum numbers  $nljm$ . The Skyrme interaction [10] is used in the p-h channel while the interaction in the particle-particle (p-p) channel is assumed to be a surface peaked density-dependent zero-range force:

$$V_{pair}(\mathbf{r}_1, \mathbf{r}_2) = V_0 \left( 1 - \frac{\rho(r_1)}{\rho_c} \right) \delta(\mathbf{r}_1 - \mathbf{r}_2) \quad (2)$$

The strength  $V_0$  is a parameter which is fixed to reproduce the odd-even mass difference of nuclei in the studied region [14].

The residual interaction in the p-h channel  $V_{res}^{ph}$  and in the p-p channel  $V_{res}^{pp}$  can be obtained as the second derivative of the energy density functional with respect to the particle density  $\rho$  and the pair density  $\tilde{\rho}$ , accordingly. Hereafter we simplify  $V_{res}^{ph}$  by approximating it by its Landau-Migdal form. For Skyrme interactions all Landau parameters with  $l > 1$  are zero. We keep only the  $l = 0$  terms in  $V_{res}^{ph}$ . In this work we study only normal parity states and one can neglect the spin-spin terms since they play a minor role [12]. The two-body Coulomb and spin-orbit residual interactions are also dropped. Therefore we can write the residual interaction in the following form:

$$V_{res}^a(\mathbf{r}_1, \mathbf{r}_2) = N_0^{-1} [F_0^a(r_1) + F_0'^a(r_1)(\tau_1 \cdot \tau_2)] \delta(\mathbf{r}_1 - \mathbf{r}_2), \quad (3)$$

where  $a$  is the channel index  $a = \{ph, pp\}$ ;  $N_0 = 2k_F m^* / \pi^2 \hbar^2$ . The expressions for  $F_0^{ph}$ ,  $F_0'^{ph}$  and  $F_0^{pp}$ ,  $F_0'^{pp}$  can be found in Ref.[17] and in Ref.[14], respectively.

The p-h matrix elements and the antisymmetrized p-p matrix elements can be written as a sum of separable terms in the radial coordinate [11, 12, 14]. Indeed, after

integrating over the angular variables one has to calculate the radial integrals,

$$I^a(j_1 j_2 j_3 j_4) = N_0^{-1} \int_0^\infty \left( F_0^a(r) + F_0^{\prime a}(r) \tau_1 \cdot \tau_2 \right) \times u_{j_1}(r) u_{j_2}(r) u_{j_3}(r) u_{j_4}(r) \frac{dr}{r^2} \quad (4)$$

where  $u_j(r)$  is the radial part of the single-particle wave function. The radial integrals (4) can be calculated accurately by choosing a large enough cut-off radius and using a  $N$ -point integration Gauss formula. Thus, the residual interaction can be expressed as a sum of  $N$  separable terms. The Hamiltonian of our method has the same form as the Hamiltonian of the well-known quasiparticle-phonon model [18], but the single-quasiparticle spectrum and the parameters of the residual interaction are calculated from the Skyrme forces.

We introduce the phonon creation operators

$$Q_{\lambda\mu i}^+ = \frac{1}{2} \sum_{jj'} \left( X_{jj'}^{\lambda i} A^+(jj'; \lambda\mu) - (-1)^{\lambda-\mu} Y_{jj'}^{\lambda i} A(jj'; \lambda - \mu) \right), \quad (5)$$

The index  $\lambda$  denotes total angular momentum and  $\mu$  is its  $z$ -projection in the laboratory system. One assumes that the ground state is the phonon vacuum  $|0\rangle$ . We define the excited states as  $Q_{\lambda\mu i}^+|0\rangle$ . Making use of the linearized equation-of-motion approach one can get the QRPA equations [15]:

$$\begin{pmatrix} \mathcal{A} & \mathcal{B} \\ -\mathcal{B} & -\mathcal{A} \end{pmatrix} \begin{pmatrix} X \\ Y \end{pmatrix} = E \begin{pmatrix} X \\ Y \end{pmatrix}. \quad (6)$$

Solutions of this set of linear equations yield the eigen energies  $E$  and the amplitudes  $X, Y$  of the excited states. The dimension of the matrices  $\mathcal{A}, \mathcal{B}$  is the space size of the two-quasiparticle configurations. Using the finite rank approximation the QRPA equations (6) can be reduced to the secular equation and the matrix dimensions never exceed  $6N \times 6N$  independently of the configuration space size [14].

We apply our approach to study characteristics of the low-lying  $2^+$  states in the even-even nuclei around  $^{132}\text{Sn}$ . We use the Skyrme interaction SLy4 [19] in the particle-hole channel together with the isospin-invariant pairing force (2). The pairing strength  $V_0$  is taken equal to  $-940 \text{ MeVfm}^3$  in connection with the soft cutoff at 10 MeV above the Fermi energies as introduced in Ref. [14].

### 3. Properties of low-lying quadrupole states

We study the  $2_1^+$  state energies and the  $B(E2 \uparrow)$ -values in  $^{126-130}\text{Pd}$ ,  $^{124-132}\text{Cd}$ ,  $^{126-134}\text{Sn}$ ,  $^{128-136}\text{Te}$ ,  $^{134-138}\text{Xe}$ . The results of our calculations [14, 20] and the available experimental data [1, 2, 4, 6, 9, 21] are shown in Fig. 1 and Fig. 2. One can

Table 1: Structure of the  $2_{1,4}^+$  states in  $^{132}\text{Te}$ .

state	$\{n_1 l_1 j_1, n_2 l_2 j_2\}_\tau$	$X$	$Y$	structure[%]
$2_1^+$	$\{2d_{5/2}, 2d_{5/2}\}_p$	0.72	0.12	25
	$\{1g_{7/2}, 2d_{5/2}\}_p$	0.30	0.05	8
	$\{1g_{7/2}, 1g_{7/2}\}_p$	0.89	0.15	39
	$\{1h_{11/2}, 1h_{11/2}\}_n$	0.55	0.20	13
$2_4^+$	$\{2d_{5/2}, 2d_{5/2}\}_p$	-0.40	0.06	8
	$\{1g_{7/2}, 2d_{5/2}\}_p$	-0.16	0.02	3
	$\{1g_{7/2}, 1g_{7/2}\}_p$	-0.54	0.08	14
	$\{1h_{11/2}, 1h_{11/2}\}_n$	1.12	0.04	63

see that there is a correct description of the isotopic and isotonic dependences. The  $2_1^+$  energies have a maximal value at  $N = 82$  for the isotopes and at  $Z = 50$  for the isotones. Such a behavior corresponds to a standard evolution of the energies near closed shells. The structural peculiarities are reflected in the evolution of the  $B(E2)$  values. The  $B(E2)$ -value at  $N = 82$  for the isotopes ( $Z = 50$  for the isotones) is either a maximal value in the Sn isotopes (the  $N = 82$  isotones), or a minimal value in the Pd, Cd, Te, Xe isotopes (the  $N = 80, 84$  isotones). As it was explained in Ref. [14, 20] the behaviour of the  $B(E2 \uparrow)$ -values is related with the proportion between the amplitudes  $X, Y$  for neutrons and protons. There is some overestimation in our calculations in comparison with the available experimental data. One can expect an improvement if the coupling with the two-phonon components of the wave functions [13] is taken into account.

Let us now discuss the structure of the  $2_1^+$  state of  $^{124-132}\text{Cd}$  and  $^{126-130}\text{Pd}$ . As shown in [20], in  $^{124-132}\text{Cd}$  the proton phonon amplitudes are dominant and the contribution of the main proton configuration  $\{1g_{9/2}, 1g_{9/2}\}$  increases from 79% in  $^{124}\text{Cd}$  to 89% in  $^{128}\text{Cd}$ , while the main neutron configuration  $\{1h_{11/2}, 1h_{11/2}\}$  exhausts about 13%, 11% and 7% of the wave function normalization in  $^{124}\text{Cd}$ ,  $^{126}\text{Cd}$  and  $^{128}\text{Cd}$ , respectively. The closure of the neutron subshell  $1h_{11/2}$  in  $^{130}\text{Cd}$  leads to the vanishing of neutron pairing and as a result the energy of the first neutron two-quasiparticle configuration  $\{2f_{7/2}, 1h_{11/2}\}$  in  $^{130}\text{Cd}$  is larger than energies of the first neutron configurations in  $^{128,132}\text{Cd}$ . It follows that in  $^{130}\text{Cd}$  the leading contribution (about 97%) comes from the proton configuration  $\{1g_{9/2}, 1g_{9/2}\}$  and the  $B(E2)$ -value is reduced. The structure of the  $2_1^+$  state of  $^{126,128,130}\text{Pd}$  is similar to that of  $^{128,130,132}\text{Cd}$ . We obtain a noncollective structure with the dominance of the proton configuration  $\{1g_{9/2}, 1g_{9/2}\}$ . In  $^{128}\text{Pd}$ , as it is discussed for  $^{130}\text{Cd}$ , the contribution of the proton  $\{1g_{9/2}, 1g_{9/2}\}$  increases to 96%. This again results in a

reduction of the  $B(E2)$  value.

The dominance of the neutron-proton attraction is one of the main features of the effective nucleon-nucleon interaction. On the other hand, the collective quadrupole isovector valence-shell excitations, so-called mixed-symmetry states [8, 22], are very sensitive to the proton-neutron interaction. That is why it is interesting to study the characteristics of the lowest isovector-collective states in nuclei around  $^{132}\text{Sn}$ . As an example we consider  $^{132}\text{Te}$ . The results of our calculation are discussed in more detail in Ref. [23]. Table 1 shows that the dominant neutron and proton phonon amplitudes  $X, Y$  of the collective  $2_1^+$  states are in phase and this corresponds to the typical isoscalar character of the lowest-lying quadrupole excitations. The next fairly collective state is the  $2_4^+$  state. The calculated energy of the  $2_4^+$  state is equal to 3.1 MeV with a calculated excitation strength of  $B(E2; 0_{gs}^+ \rightarrow 2_4^+) = 330 e^2\text{fm}^4$ . The dominant neutron and proton amplitudes of the  $2_4^+$  state are in opposite phase. The isovector character of the  $2_4^+$  is reflected in the noticeable size of the  $B(M1; 2_4^+ \rightarrow 2_1^+)$  value equal to  $0.25\mu_N^2$ . This analysis can help to identify the mixed-symmetry states in  $^{132}\text{Te}$ , but it is only a rough estimate since the effects of the phonon-phonon coupling are not considered.

## 4. Conclusions

A finite rank separable approximation for the QRPA calculations with Skyrme-type interactions is presented. This approach enables one to reduce remarkably the dimensions of the matrices that must be diagonalized to perform structure calculations in very large configuration spaces. Using the same set of parameters we have investigated the evolution of the  $2_1^+$  state energies and the  $B(E2)$ -values in  $^{126-130}\text{Pd}$ ,  $^{124-132}\text{Cd}$ ,  $^{126-134}\text{Sn}$ ,  $^{128-136}\text{Te}$ ,  $^{134-138}\text{Xe}$ . Our calculations for the energies and the  $B(E2)$ -values describe correctly the isotopic and isotonic dependences. We give predictions for the structure of the  $2_1^+$  state in  $^{126-130}\text{Pd}$ ,  $^{124-132}\text{Cd}$ . As an illustration of the method we study the lowest isovector collective quadrupole state in  $^{132}\text{Te}$ . It is found from our calculations that the  $2_4^+$  state might be the best candidate for the mixed-symmetry state. To finalize the study one needs to take into account the phonon-phonon coupling.

## Acknowledgments

We are grateful to Prof. R. V. Jolos and Prof. Ch. Stoyanov for useful discussions. This work was supported in parts by the Heisenberg-Landau program and by the IN2P3-JINR agreement.

[1] D. C. Radford *et al.*, Phys. Rev. Lett. **88**, 222501 (2002).

- [2] G. Jakob *et al.*, Phys. Rev. C **65**, 024316 (2002).
- [3] A. Scherillo *et al.*, Phys. Rev. C **70**, 054318 (2004).
- [4] D. C. Radford *et al.*, Nucl. Phys. **A752**, 264c (2005).
- [5] H. von Garrel *et al.*, Phys. Rev. C **73**, 054315 (2006).
- [6] A. Jungclaus *et al.*, Phys. Rev. Lett. **99**, 132501 (2007).
- [7] M. Dworschak *et al.*, Phys. Rev. Lett. **100**, 072501 (2008).
- [8] N. Pietralla, P. von Brentano, A. F. Lisetskiy, Prog. Part. Nucl. Phys. **60**, 225 (2008) and references cited therein.
- [9] L. Cáceres *et al.*, Phys. Rev. C **79**, 011301 (2009).
- [10] D. Vautherin, D. M. Brink, Phys. Rev. C **5**, 626 (1972).
- [11] Nguyen Van Giai, Ch. Stoyanov, V.V. Voronov, Phys. Rev. C **57**,1204 (1998).
- [12] A. P. Severyukhin, Ch. Stoyanov, V. V. Voronov, Nguyen Van Giai, Phys. Rev. C **66**, 034304 (2002).
- [13] A. P. Severyukhin, V. V. Voronov, Nguyen Van Giai, Eur. Phys. J. A **22**, 397 (2004).
- [14] A. P. Severyukhin, V. V. Voronov, Nguyen Van Giai, Phys. Rev. C **77**, 024322 (2008).
- [15] P. Ring, P. Schuck, *The Nuclear Many Body Problem* (Springer, Berlin, 1980).
- [16] J. P. Blaizot, D. Gogny, Nucl. Phys. A **284**, 429 (1977).
- [17] Nguyen Van Giai, H. Sagawa, Phys. Lett. B **106**, 379 (1981).
- [18] V. G. Soloviev, *Theory of Atomic Nuclei: Quasiparticles and Phonons* (Institute of Physics, Bristol and Philadelphia, 1992).
- [19] E. Chabanat *et al.*, Nucl. Phys. A **635**, 231 (1998).
- [20] A. P. Severyukhin, V. V. Voronov, Nguyen Van Giai, Phys. At. Nucl. **72**, 1787 (2009).
- [21] S. Raman, C. W. Nestor Jr., P. Tikkanen, At. Data Nucl. Data Tables **78**, 1 (2001).
- [22] F. Iachello, Phys. Rev. Lett. **53**, 1427 (1984).
- [23] A. P. Severyukhin, N. N. Arsenyev, V. V. Voronov, N. Pietralla, Nguyen Van Giai, in preparation.

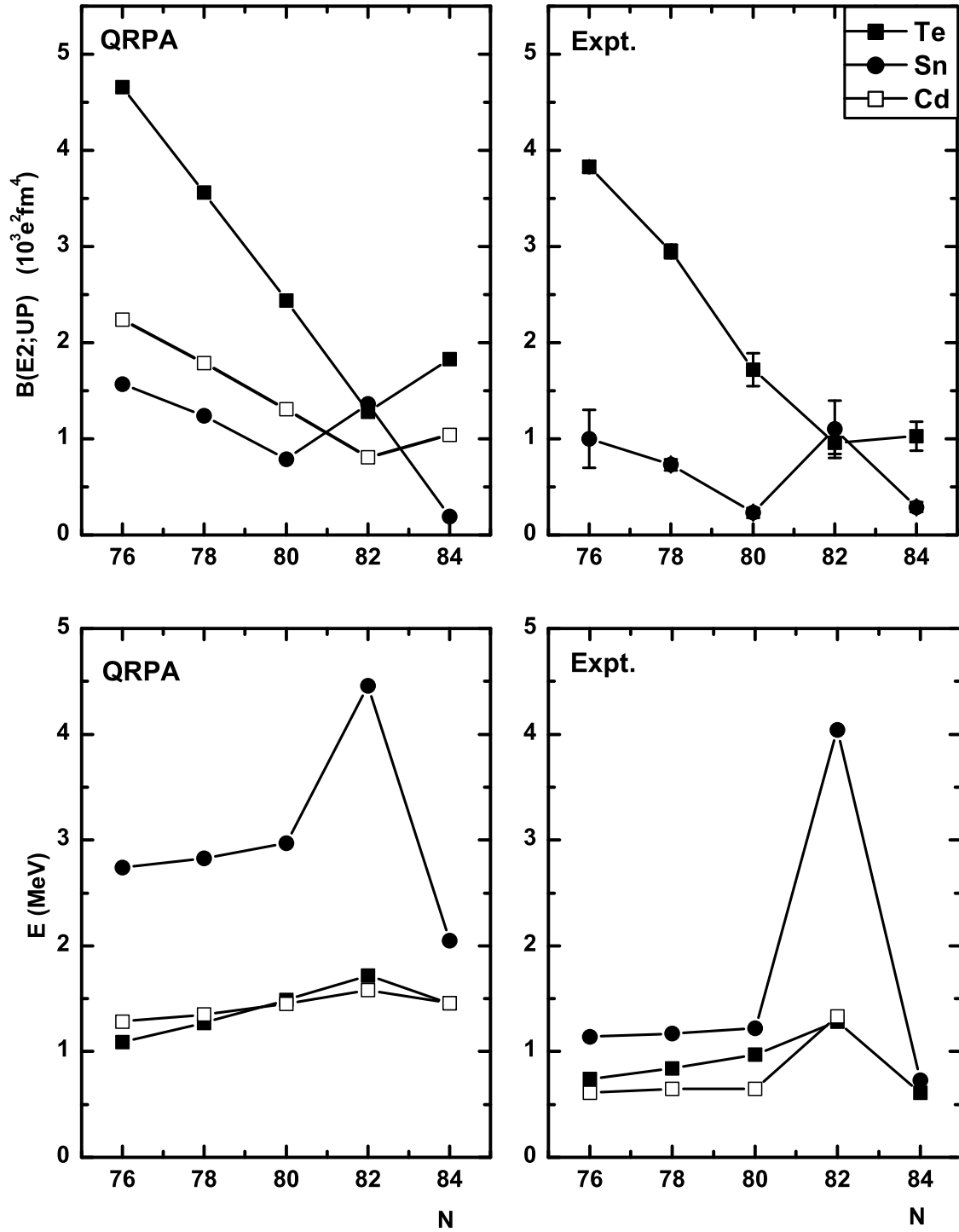


Figure 1: Energies and  $B(E2;0_{gs}^+ \rightarrow 2_1^+)$  values of  $2_1^+$  states in  $^{124-132}\text{Cd}$ ,  $^{126-134}\text{Sn}$ ,  $^{128-136}\text{Te}$ . Results of the QRPA calculations are represented in the left panels; the available experimental data are in the right panels.

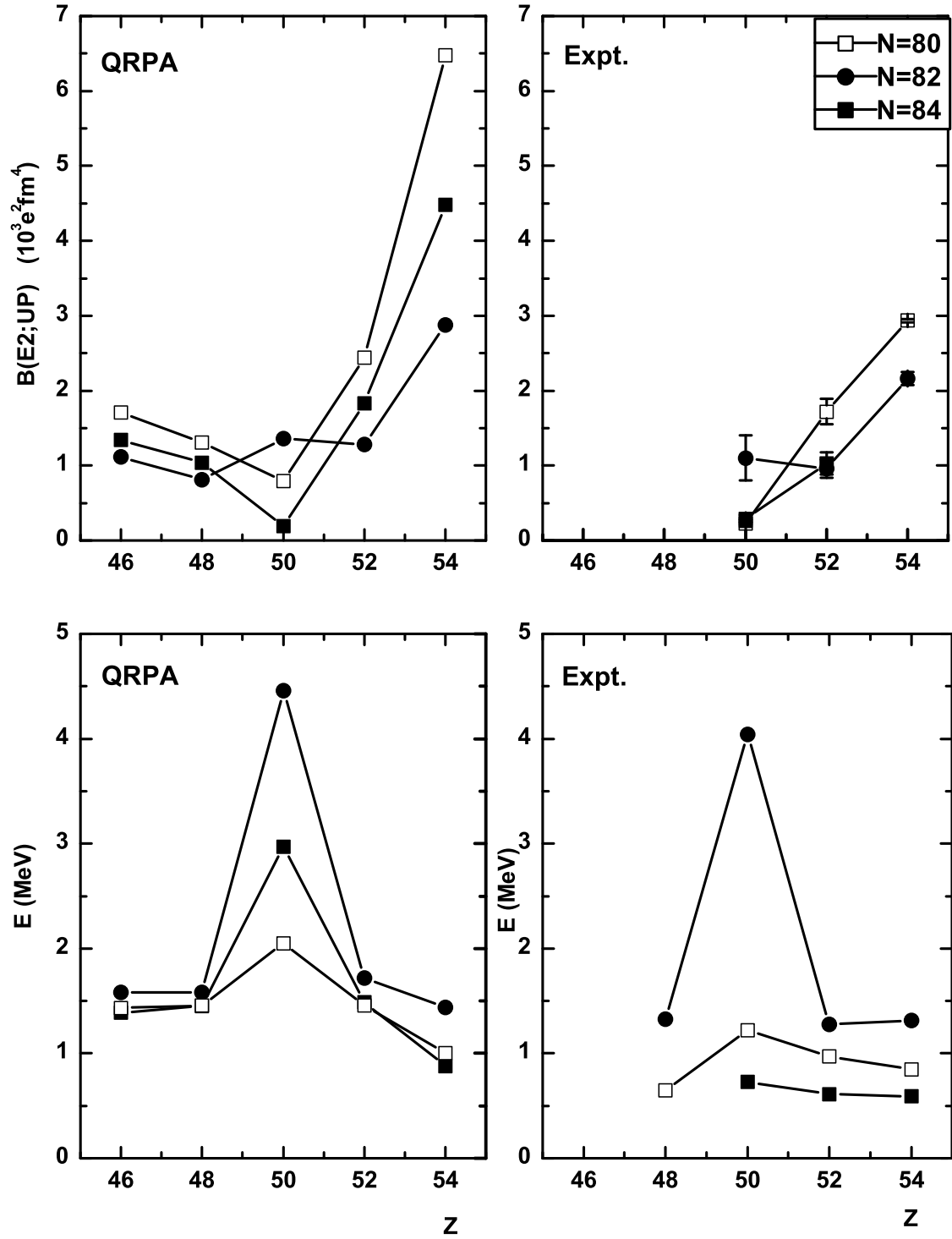


Figure 2: Energies and  $B(E2; 0_{gs}^+ \rightarrow 2_1^+)$  values of  $2_1^+$  states in the  $N = 80, 82, 84$  isotones. Results of the QRPA calculations are represented in the left panels; the available experimental data are in the right panels.